FRIGID ZONE **MEDICINE**
Original Article • DOI: 10.2478/fzm-2023-0029

Cold exposure promotes coronavirus infection by altering the gut microbiota and lipid metabolism to reduce host immunity

Gaosong Wu[1#], Yuhao Zhang[1,2#], Ningning Zheng[3], Saisai Tian[4], Jingyu Liao[1], Wanqi Le[1], Houkai Li[2*], Weidong Zhang[1,2,4,5*]

Abstract

Objective: Cold exposure has been suggested to be advantageous for the spread and infection of the coronavirus, and the gut microbiota influences the severity of the infection by modulating host inflammatory and immune responses. However, it remains unclear whether the promotion of viral infection through cold exposure is linked to the gut microbiota. **Methods:** In this study, we performed an unbiased analysis of gut microbiota, serum, and lung tissue metabolome changes in cold-exposed and virus-infected mice, alongside the assessment of immune-inflammatory indicators in serum and lung tissue. **Results:** The results revealed that both cold exposure and viral infection significantly decreased the percentage of peripheral blood lymphocytes ($CD4^+$ T cells, $CD8^+$ T cells, and B cell) and increased the expression of inflammatory factors (IL-6, IL-1β, TNF-α, and IFN-γ). Meanwhile, cold exposure disrupted the homeostasis of gut microbiota, elevating the abundance of pathogenic bacteria (*Staphylococcus*) and diminishing the abundance of beneficial bacteria (*Alistipes*). Notably, in virus-infected mice exposed to a cold environment, the reduction in the abundance of beneficial bacteria *Alistipes* was more pronounced than in cases of single virus infection and cold exposure. Analysis of altered serum and lung tissue metabolites highlighted glycerophospholipids, fatty acids, and eicosanoids as the most affected metabolites by cold exposure. These metabolites, closely associated with virus infection, exhibited a significant correlation with immune-inflammatory indicators. **Conclusion:** These findings establish a mechanistic connection between cold exposure and virus infection, suggesting that cold exposure-induced dysregulation of gut microbiota and lipid metabolism diminishes host immunity, promoting virus infection.

Keywords

cold exposure; coronavirus infection; gut microbiota; lipid metabolism; immune

Received 18 October 2023, Accepted 21 November 2023

[1]*Institute of Interdisciplinary Integrative Medicine Research, Shanghai University of Traditional Chinese Medicine, Shanghai 201203, China*
[2]*School of Traditional Chinese Pharmacy, China Pharmaceutical University, Nanjing 211198, China*
[3]*School of Pharmacy, Shanghai University of Traditional Chinese Medicine, Shanghai 201203, China*
[4]*Department of Phytochemistry, School of Pharmacy, Second Military Medical University, Shanghai 200433, China*
[5]*Institute of Medicinal Plant Development, Chinese Academy of Medical Sciences & Peking Union Medical College, Beijing 100193, China*

**Corresponding authors Houkai Li, E-mail: hk_li@shutcm.edu.cn; Weidong Zhang, E-mail: wdzhangy@hotmail.com*
[#]These authors contributed equally to this work.

1 Introduction

As we entered the 21st century, several coronavirus pandemics, notably the 2019 novel coronavirus (SARS-CoV-2), severe acute respiratory syndrome (SARS-CoV), Middle East respiratory syndrome (MERS-CoV), and influenza A viruses (H1N1 and H3N2 strains), have posed an unprecedented threat to global health and lives[1]. Innate immunity, acting as the first line of defense against viral invasions underscores the critical role immune cells play in reshaping metabolic pathways to fulfill energy and biosynthesis demands during activation[2]. Notably, individuals with compromised immune states face the highest risk of mortality from coronavirus infections[3]. Immune cells reshape metabolic pathways to meet the need for energy and biosynthesis demands during activation[4]. Maintaining immunity and immune surveillance necessitates a substantial allocation of metabolic resources. Exposure to cold environments, aimed at reducing heat dissipation and increasing heat production, triggers a high-cost, high-gain physiological response. However, this elevated energy demand may potentially compete with the immune system[5]. Recent epidemiological evidence highlights that exposure to a cold environment can expedite the infection and transmission of coronaviruses[6]. Consequently, cold exposure emerges as intricately linked to coronavirus infection, although the precise mechanisms remain unclear.

The interaction between gut microbiota and the host in the context of coronavirus infection has been extensively studied[7-9]. Notably, the severity of coronavirus infection is linked to the regulation of host inflammatory and immune responses the gut microbiota[10-11]. Hyperactive inflammatory and immune responses during or after SARS-CoV-2 infection were closely associated with an imbalance of gut microbiota homeostasis[12]. SARS-CoV-2 infection has been shown to induce damage to the gut epithelium, leading to the translocation of gut opportunistic pathogens and endotoxins. This process exacerbates systemic inflammatory responses, increasing the risk of secondary infection, acute respiratory distress syndrome, multiple organ failure, and mortality[13-14]. Moreover, the gut microbiota plays a pivotal role in coordinating overall energy homeostasis during cold exposure[15]. Meanwhile, cold exposure influences the immune system, impairing extracellular vesicle swarm mediated nasal antiviral immunity[16] and protecting from neuroinflammation through immunologic reprogramming[5]. Given these findings, we hypothesize that cold exposure may disrupt gut microbiota homeostasis and affect immune function, potentially promoting viral infection.

In this study, we constructed mouse models exposed to cold conditions and infected with a virus. Using 16S rRNA sequencing and metabolomics analysis *via* liquid chromatography-tandem mass spectrometry (LC-MS), we delved into the intricate interplay between gut microbiota, host metabolism, and the immune system. Our findings indicate that immune system alterations induced by cold exposure are intricately linked to the reprograming of gut microbiota and host metabolism. Cold exposure emerges as a factor capable of promoting coronavirus infection and exacerbating its impact on the host's immune system. This effect is likely mediated by the disruption of gut microbiota and perturbation of host lipid metabolism.

2 Materials and methods

2.1 Materials and chemicals

Human coronavirus 229E (HCoV-229E) (Institute of Medicinal Biotechnology Chinese Academy of Medical Sciences, Beijing, China), SPF grade BALB/c mice (10-12 g) (HFK Bioscience Co., Ltd., Beijing, China),interferon (IFN-γ), tumor necrosis factor (TNF-α), interleukin (IL-1β) and IL-6 ELISA kits (Bio-Techne Corporation, Minnesota, USA), APC anti-mouse CD8a (53-6.7), anti-mouse CD4 (RM4-5), PE anti-mouse CD19 (1D3) antibodies and RBC Lysis Buffer (10X) (TONBO Biosciences, California, USA), acetonitrile, water, methanol, and formic acid (LC-MS grade) (Fisher Scientific, Massachusetts, USA), EZNA soil DNA kit (Omega Bio-Tek, Georgia, USA). The study was approved and monitored by the Animal Care and Use Committee of the Institute of Chinese Materia Medica, China Academy of Chinese Medical Sciences (2020D028).

2.2 Establishment of animal models for cold exposure and coronavirus infection

Following one week of adaptive feeding, 40 mice were randomly assigned to 4 groups (N = 10): the control (Con) group, cold-humid exposure (CH) group, virus infection (VI) group, and cold-humid environment combined with virus infection (CH_VI) group. Mice in the CH and CH_VI groups were maintained in an artificial climate box with relative humidity of 90% ± 3% and a temperature of 4 ± 2°C for 4 hours daily over ten consecutive days. In the VI and CH_VI groups, mice were infected with 50 μL of HcoV-229E (100TCID50) using the nose-dripping method after being anaesthetized with isoflurane (infection occurred on the 6th and 7th day). The Con and CH groups were infected with a culture solution lacking HcoV-229E for four consecutive days (Fig. 1A).

2.3 Histological analysis and HCoV-229E detection in lung tissue

For histological analysis, lung tissues were fixed in 10% neutral formalin for 48 h. Following dehydration and paraffin embedding, hematoxylin-eosin H & E staining was performed using a standardized process. Representative images were observed and captured using an electron microscope. To detect the r viral load, lung tissue was ground into powder with a pestle in a mortar. Liquid nitrogen was added during the process. The resulting powder was placed in a 1.5-mL centrifuge tube, and 1 mL of TRIzol reagent was added. The viral load of mice was determined following the standard operating procedure of the kit (HCoV-229E Real Time PCR kit, Shanghai ZJ Bio-Tech Co., Ltd., China).

2.4 Peripheral blood lymphocytes and inflammatory cytokine detections

Peripheral blood lymphocytes, including $CD4^+$ T cells and $CD8^+$ T cells and B cells, analyzed using flow cytometry. The detailed method was based on our previous publications[17]. For inflammatory cytokines in lung tissue, 50 mg of lung tissue was added to 500 μL of normal saline, homogenized, and centrifuged to obtain the supernatant. IL-6, IL-1β, TNF-α, and IFN-γ were detected following the instructions provided by the ELISA kit manufacturer.

2.5 Metabolomics study based on HPLC-QTOF-MS/MS

For serum samples, 50 μL of serum was thawed and mixed with ice-cold MeOH: ACN (150 μL, 1: 1) for protein precipitation. After

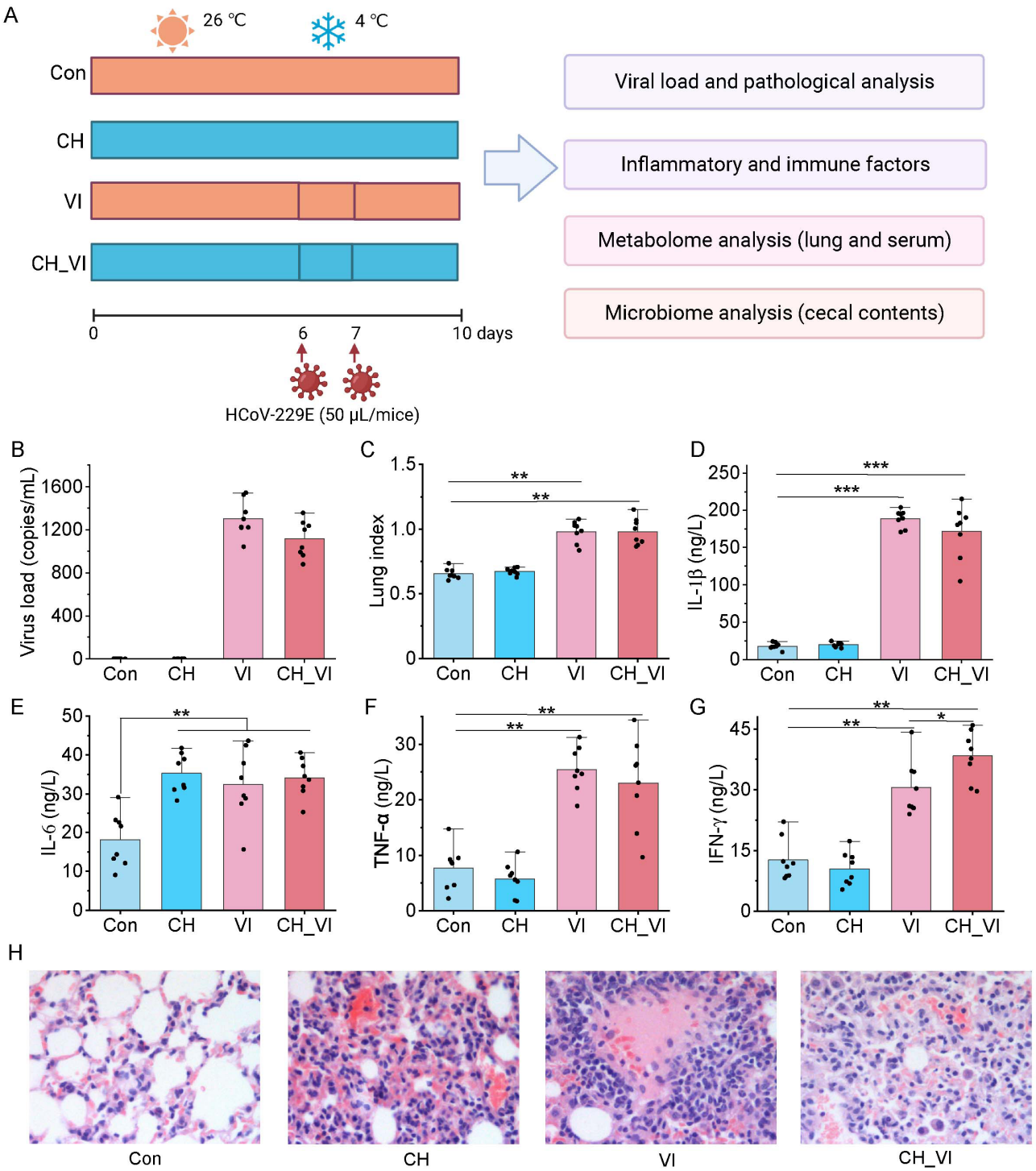

Fig. 1 Phenotypic changes in cold-exposed and virus-infected mice. Con, control group; CH, cold humid exposure group; VI, virus infection group; CH_VI, cold humid environment combined with virus infection group. (A) Experimental process; (B) Viral load detection; (C) Lung index; (D-G) The levels of inflammatory cytokines in lung tissue (IL-1β, IL-6, TNF-α, and IFN-γ); (H) Lung histopathological photographs (H&E staining). Significance was evaluated by one-way ANOVA, follow by Dunnett's multiple comparisons test. *, $P < 0.05$; **, $P < 0.01$; ***, $P < 0.001$; $N = 8$ each group.

vortex for 30 s and subsequent ultrasonication for 10 min in an ice bath, the sample was placed in a -20°C refrigerator overnight to enhance protein precipitation. The supernatant was obtained by centrifugation at 12, 000 rpm for 15 min at 4°C, and 2 μL of the supernatant was used for further LC-MS/MS analysis. For lung tissues, 10 mg of tissue was homogenizer with 200 μL of water, and 800 μL of MeOH: ACN (1: 1, *v/v*) was added for protein precipitation. After vortex (30 s) and ultrasonication (10 min) in an ice bath, the sample was placed in a -20°C refrigerator overnight. After centrifugation (12, 000 rpm, 15 min), the supernatant was transferred into a clean, dry tube, dried with nitrogen, and the residue was dissolved with ACN: H2O (1: 1, *v/v*). After centrifugation (12, 000 rpm, 15 min), the supernatant was obtained for LC-MS/MS analysis. Sample analysis was performed by High-resolution mass spectrometry (SCIEX Triple TOF 5600$^+$) in tandem with a Shimadzu HPLC system (Nexera XR LC-20AD) was used for sample analysis. For more detailed information on the procedures, including chromatographic columns and instrument parameter settings, please refer to our previous publications[18].

The wiff data were imported into Progenesis QI for peak alignment to obtain a list of the peaks, and the identification of metabolites was achieved based on the online databases, including the METLIN (https: //metlin.scripps.edu/), LIPIDMAPS (https: //www.lipidmaps.org/), HMDB (https: //hmdb.ca/), and KEGG (https: //www.genome.jp/). The metabolites with FDR < 0.05 were selected as differential metabolites (DMs) for further statistical analyses.

2.6 Fecal microbiota 16S rRNA sequencing

Microbial genomic DNA was extracted from fecal samples using the EZNA® soil DNA kit (Omega Bio-tek, USA) following the manufacturer's protocol. Qualified DNA samples were utilized for the amplification of the 16S rDNA V3-V4 region using the universal primers 338F and 806R. For more detailed information, refer to our previous publications[18].

2.7 Statistical analysis

Apart from the detailed 16S rRNA data, other data are shown as means ±SEM. All statistical analyses were carried out using IBM SPSS software 25.0. Differences between two groups were assessed using Student's *t*-test, while more than two groups were evaluated by one-way analysis of variance (ANOVA). $P < 0.05$ was considered statistically significant.

3 Results

3.1 Effect of cold exposure on the expression of inflammatory factors in mice

To assess the impact of cold exposure on HCoV-229E infection severity in lung tissue, we initially detected the nucleic acid of HCoV-229E. Our results revealed comparable levels of HCoV-229E nucleic acid in both VI and CH_VI groups (Fig. 1B). This finding was consistent with the lung index data (Fig. 1C). Subsequently, we measured inflammatory factors in lung tissue and observed a significant increase in levels, including TNF-α, IL-1β, IL-6, and IFN-γ, due to viral infection (VI *vs.* Con, $P < 0.01$ or $P < 0.001$). Subsequently, we measured inflammatory factors in lung tissue and observed a significant increase in the levels of TNF-α, IL-1β, IL-6, and IFN-γ (VI *vs.* Con, $P < 0.01$ or $P < 0.001$). In contrast, cold exposure only increased the expression of IL-6 (CH *vs.* Con, $P < 0.01$), and no significant differences in inflammatory factors (such as IL-1β, IL-6 and TNF-α) were observed between VI and CH-VI groups, except for IFN-γ (CH-VI *vs.* VI, $P < 0.05$) (Fig. 1D–G).

These results suggest that viral infection notably promotes the inflammatory response in mice, while the impact of cold exposure on the inflammatory response is limited. Further pathological analysis of lung tissue also confirmed our findings. Cold exposure caused induced lung tissue damage, characterized by proliferative cells, lymphocyte infiltration, red blood cells exudation, and extensive mucus production. Inflammatory reactions and engorgement were observed in the vasculature around the bronchiole. Intriguingly, cold exposure did not aggravate the damage to lung tissue induced by VI. Similar degrees of damage, including substantial alveolar fusion, blood stasis leaking in pulmonary interstices, noticeable tissue edema and hyperplasia, and significant pulmonary interstitial inflammation, were observed in both VI and CH_VI groups (Fig. 1H).

3.2 Cold exposure aggravates deterioration of the immune system in virus-infected mice

The immune system's pivotal role in the combating viral infections is undeniable. To elucidate the adverse effects of cold exposure on the immune system, we analyzed peripheral blood lymphocytes using flow cytometry. As depicted in Fig. 2, we observed a significant decreased in the levels of CD4$^+$ T cells and CD8$^+$ T cells due to cold exposure (CH *vs.* Con, $P < 0.05$ or $P < 0.01$). A similar trend was also evident in virus-infected mice (VI *vs.* Con, $P < 0.01$). Notably, viral infection exhibited a more pronounced reduction in CD4$^+$ T cells and CD8$^+$ T cells compared to cold exposure alone. Interestingly, while cold exposure and viral infection did not individually reduce the percentages of B cells, their simultaneous stimulation led to a significant reduction in B cell percentages (CH_VI *vs.* Con, $P < 0.05$). Importantly, we found that the combined stimulation of cold exposure and viral infection had a more significant reduction effect on the percentage of CD4$^+$ T cells and CD8$^+$ T cells in peripheral blood than single stimulation

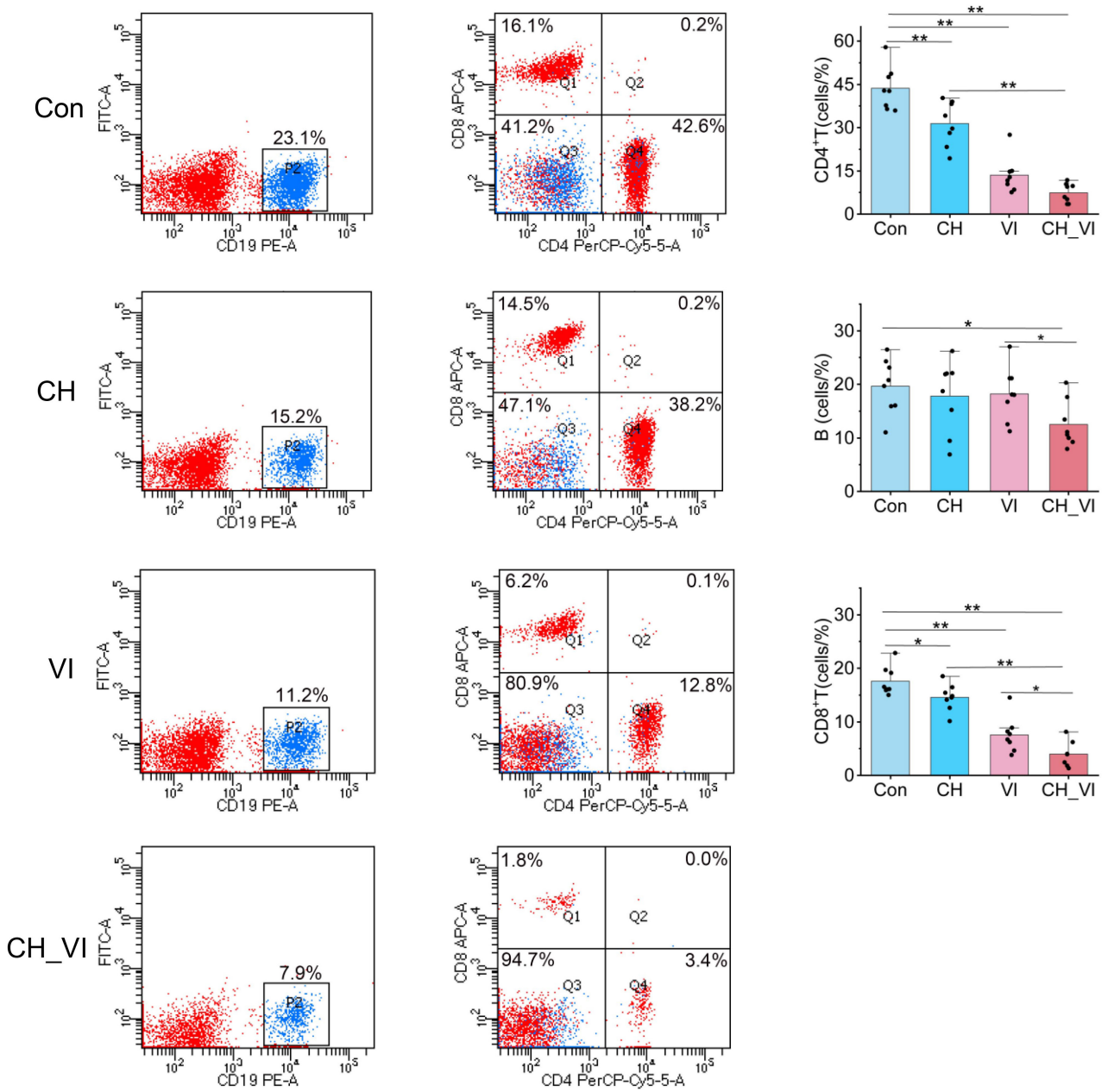

Fig. 2 The levels of peripheral blood lymphocyte ($CD4^+$- and $CD8^+$-T cells and B cells) in cold exposure and viral infection mice. Significance was evaluated by one-way ANOVA, follow by Dunnett's multiple comparisons test. *, $P < 0.05$; **, $P < 0.01$; $N = 8$ each group.

(CH_VI *vs.* Con, $P < 0.01$). These results underscore that cold exposure exacerbates the impairment of immune function caused by viral infection.

3.3 Cold exposure alters the gut microbiota composition in virus-infected mice

The gastrointestinal tract, considered the body's largest immune organ, relies on its resident microbiota to regulate host immunity, defend against pathogens, and support nutrient functions[19]. Our investigation aimed to ascertain whether cold exposure, by affecting the composition of the gut microbiota, could potentially harm the immune system. Analysis of 16S rRNA sequencing results revealed that cold exposure induced changes in the alpha diversity of the gut microbiota, exhibiting lower richness and diversity at the genus level compared to the Con group (Fig. 3A–B).

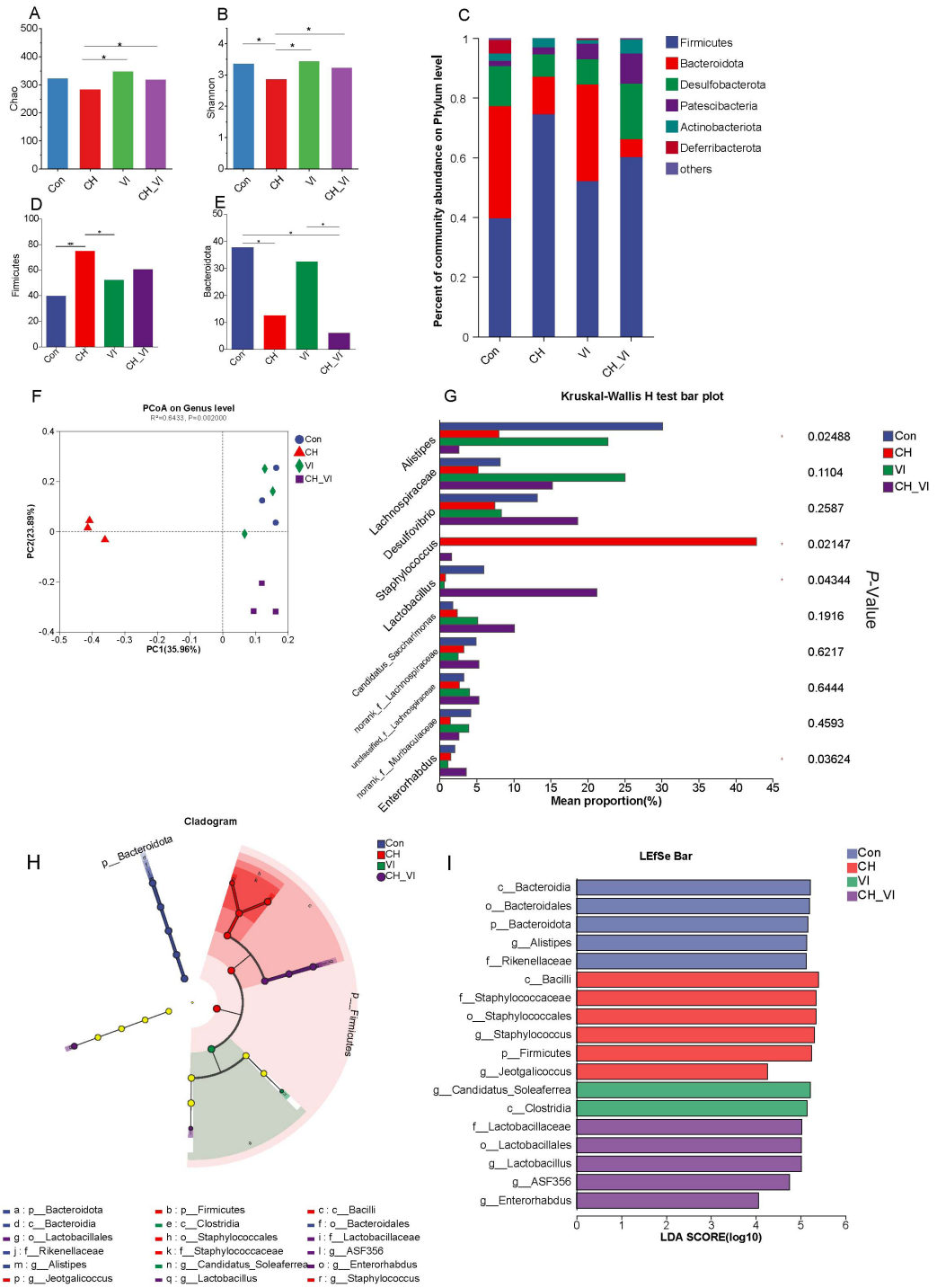

Fig. 3 Analysis of gut microbiota structure in mice subject to cold exposure and virus infection. Con, control group; CH, cold humid exposure group; VI, virus infection group; CH_VI, cold humid environment combined with virus infection group. (A-B) α diversity analysis (Chao and Shannon) at the genus level; (C) Bar chart showing the phylum-levels composition of the gut microbiome; (D-E) Changes in the abundance of *Firmicute*s and Bacteroidota in mice subjected to cold exposure and virus infection; (F) Principal coordinates analysis (PCoA) based on genus level; (G) Genus level multi-group comparison chart; (H) Cladogram visualizing the output of the LEfSe analysis; (I) The most significant difference of gut microbial taxa among groups after LDA (LDA > 4). The abbreviations are as follows: p, phylum; c, class; o, order; f, family; and g, genus. *, $P < 0.05$; **, $P < 0.01$; $N = 3$ each group.

At the phylum level, *Firmicute*, *Bacteroidota* and *Desulfobacterota* emerged as the three most abundant species (Fig. 3C). Notably, in the CH group, *Firmicute* levels were higher than those in the Con group, while *Bacteroidota* were lower. These changes were also observed in the VI and CH_VI groups, albeit not as prominently as in the CH group (Fig. 3D–E). To assess the degree of similarity between microbial communities, β-diversity was further evaluated using Bray-Curtis principal co-ordinates analysis (PCoA) plot, at genus level. The results illustrated a distinct separation trend between the CH, CH-VI, and the Con groups, indicating differences in the gut microbiota structure (Fig. 3F). Furthermore, the Kruskal Wallis H test was employed to analyze the top 10 bacteria at the genus level, revealing significant changes in *Alistipes*, *Staphylococcus*, *Lactobacillus* among the four groups (Fig. 3G).

To discern the specific bacterial from phylum to genus associated with the Con, CH, VI, and CH_VI groups, LDA and LEfSe analyses were performed to pinpoint the most remarkable taxa explaining differences between groups. As depicted in Fig. 3H–I, we identified d 18 specific bacterial (LDA > 4) across four groups, encompassing 7 genera. The Con group exhibited a predominance of *Alistipes* at the genus level. In contrast, the CH group featured the genera *Staphylococcus* and *Jeotgalicoccus*. *Alistipes* is a potential bacterium known to regulates the inflammatory response[20]. *Staphylococcus*, on the other hand, is a major contributor to health burden, known for its impact on the immune system adaptive immune response features and bacterial escape mechanisms[21]. Given its resistance to vaccine development, *Staphylococcus* stands as a significant health burden[22]. Therefore, changes in these bacteria may be closely related to the occurrence and progression of diseases caused by cold exposure. In the VI group, *Candidatus Soleaferrea* emerged as the dominant bacteria, while the CH-VI group was characterized by dominance from *Lactobacillus*, ASF356 and *Enterorhabdus*. *Candidatus Soleaferrea* is recognized as a beneficial bacterium that produces anti-inflammatory effects by secreting metabolites to maintain intestinal homeostasis[23-24]. *Enterorhabdus* has been associated with mucosal inflammation in mice[25]. Consequently, these bacteria may play a role in the effects of cold exposure and viral infection on the immune system. In order to further compare the differences in bacteria among each group, we analyzed the differences of the top 10 bacteria at the genus level based using Student's *t*-test (Fig. 4). In comparison to the Con group, the abundance of *Staphylococcus* significantly increased ($P < 0.01$), while the abundance of *Alistipes* significantly decreased ($P < 0.05$) in the CH group (Fig. 4A). Additionally, in the CH_VI group compared to the Con group, we observed a significant decrease in *Alistipes* ($P < 0.05$) and a significant increase in *Lactobacillus* ($P < 0.05$) (Fig. 4C). However, no significant difference in the abundance of the top10 bacteria was found between the VI and Con groups (Fig. 4B). These findings indicated that cold exposure plays a key role in inducing structural imbalance in the gut microbiota of virus-infected mice.

3.4 Cold exposure alters the lung metabolome in virus-infected mice

In the lung metabolome, we identified 211 differential ions (including 97 upregulated and 112 downregulated ions) between the CH and Con groups, 345 differential ions (including 221 upregulated and 124 downregulated ions) between the VI and Con groups, and 327 differential ions (including 210 upregulated and 117 downregulated ions) between the CH_VI and Con groups (Fig. 5A–C). These results indicate that viral infection induces more pronounced metabolic disturbances in lung tissue than cold exposure. Progenesis QI identified a total of 120 DMs based on HMDB, KEGG, LIPIDMAPS, and METLIN databases (Supplementary Table S1) displaying common and independent DMs among the four groups as in Fig. 5D. The principal component analysis (PCA) model based on these 120 DMs effectively separates the four groups (Fig. 5E).

As illustrated in Fig. 5F, there are distinctions in the types of metabolites affected by cold exposure and viral infection. Cold exposure primarily affects glycerophospholipids, fatty acids, carbohydrates, and eicosanoids, while viral infection predominantly impacts amino acids, carbohydrates, nucleosides, glycerophospholipids, fatty acids, and eicosanoids. In Fig. 5G, cold exposure mainly causes the upregulation of glycerophospholipids and the downregulation of fatty acids. Conversely, virus infection results significant changes in various metabolite types, including the upregulation of amino acids, carbohydrates, glycerophospholipids, nucleosides, and eicosanoids, along with the downregulation of fatty acids. Correlation chord diagrams further illustrate that viral infection leads to more complex metabolite changes in lung tissue compared to cold exposure, with a superimposed effect between the two (Fig. 5H–J).

3.5 Cold exposure alters the serum metabolome in virus-infected mice

In contrast to the lung metabolome results, cold exposure exhibited a more pronounced impact on the serum metabolome than the viral infection group. Within the serum metabolome, we identified 100 differential ions (including 20 upregulated and 80 downregulated ions) between the CH and Con groups, 47 differential ions (including 12 differential ions were upregulated and 35 differential ions were downregulated) between the VI and Con groups, and 200 differential ions (including 82 upregulated and 118 downregulated ions) between the CH_VI and Con

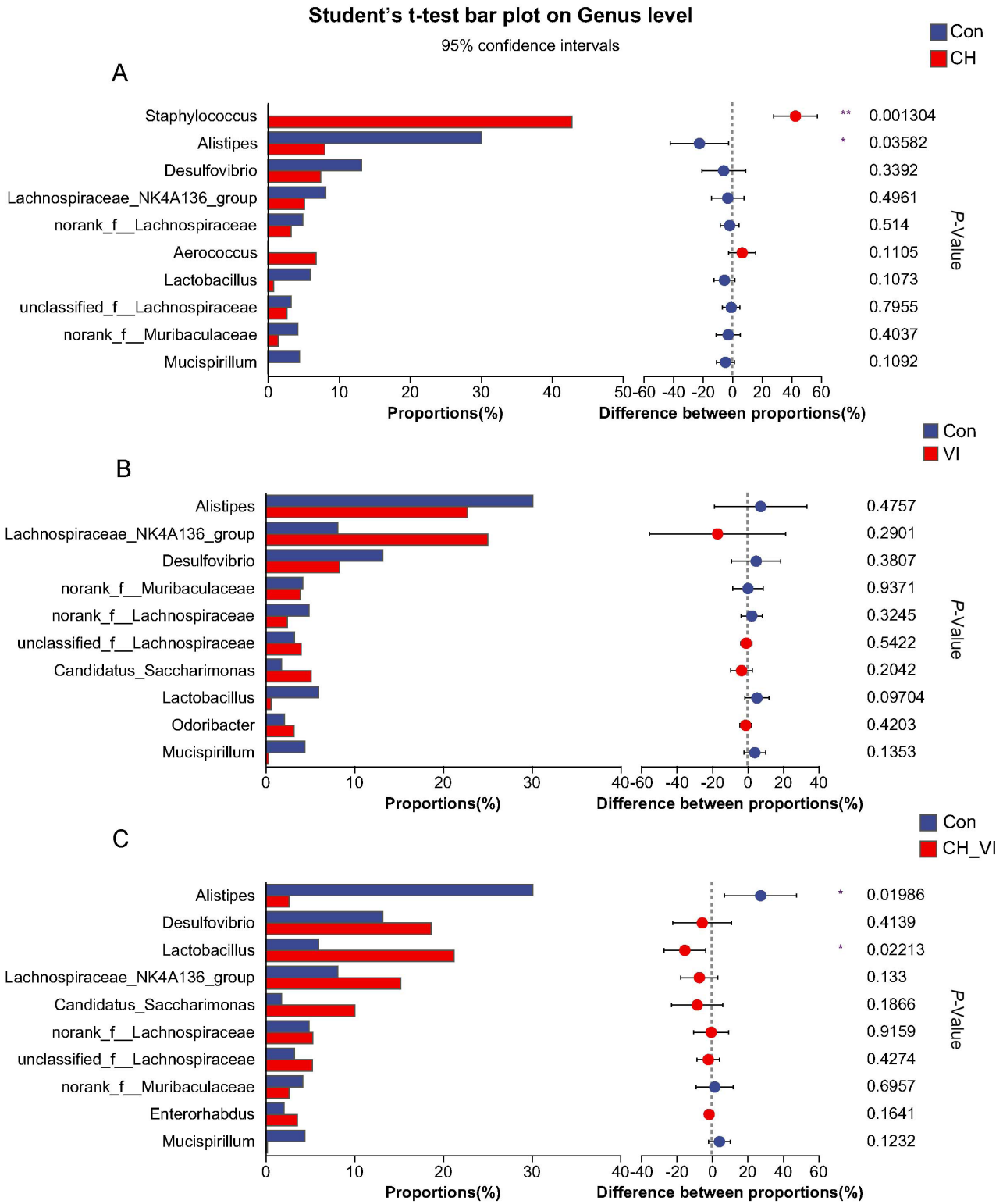

Fig. 4 Species difference analysis based on genus level. Con, control group; CH, cold humid exposure group; VI, virus infection group; CH_VI, cold humid environment combined with virus infection group. (A) CH *vs.* Con; (B) VI *vs.* Con; (C) CH_VI *vs.* Con. $N = 3$ each group.

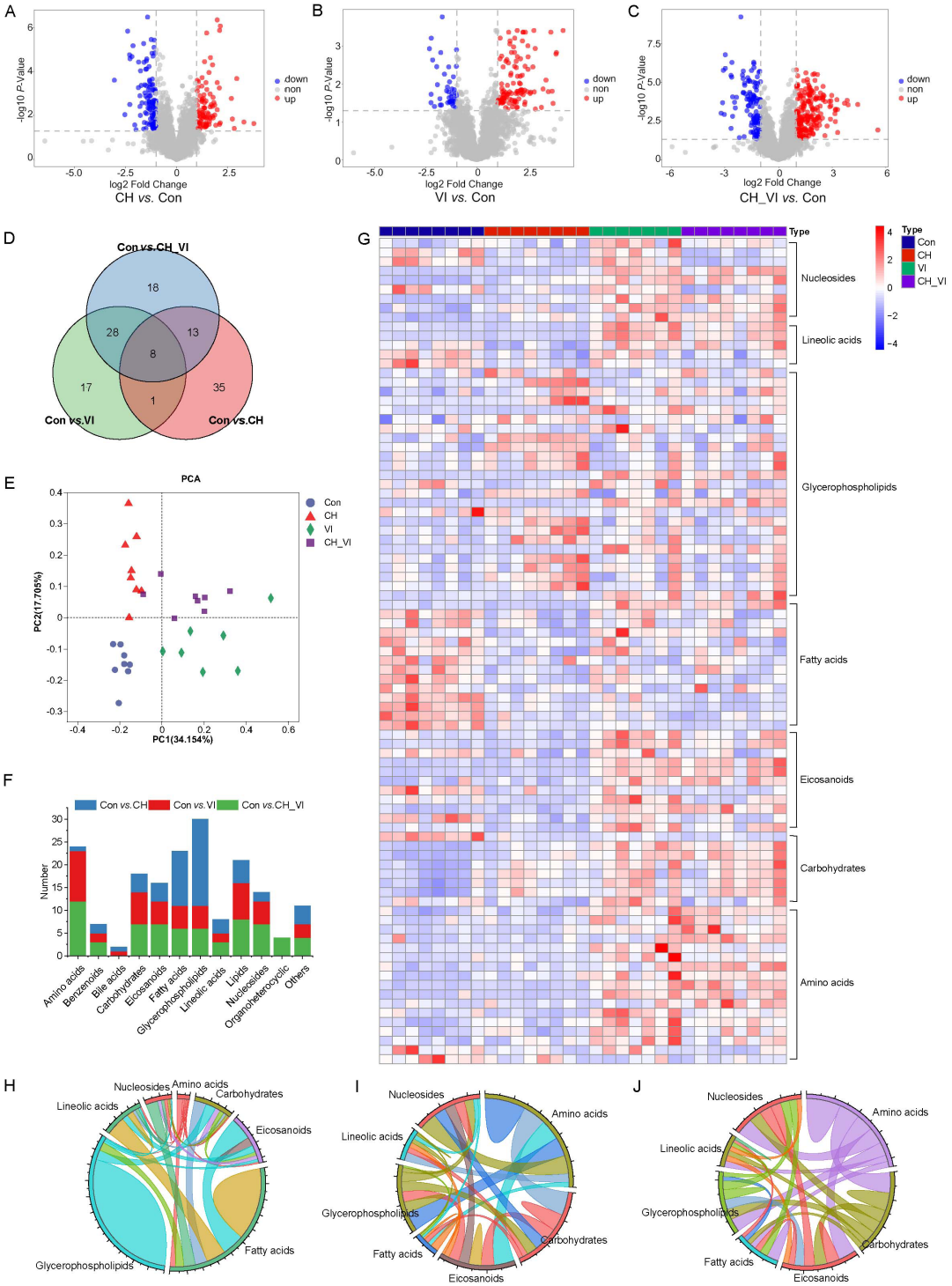

Fig. 5 Metabolome analysis of lung tissue specimens. Con, control group; CH, cold humid exposure group; VI, virus infection group; CH_VI, cold humid environment combined with virus infection group. (A-C) Volcano plot showing changes in differential ions between CH, VI, CH_VI and Con group; (D) Venn diagram of DMs in the Con, CH, VI and CH_VI groups; (E) The PCA plots established based on DMs in the Con, CH, VI and CH_VI groups; (F) The categories and number of DMs obtained from the Con, CH, VI and CH_VI groups; (G) Heatmap diagram of DMs in the Con, CH, VI and CH_VI groups; (H) The DMs correlation between major DMs classes in the CH group; (I) The DMs correlation between major DMs classes in the VI group; (J) The DMs correlation between major DMs classes in the CH_VI group.

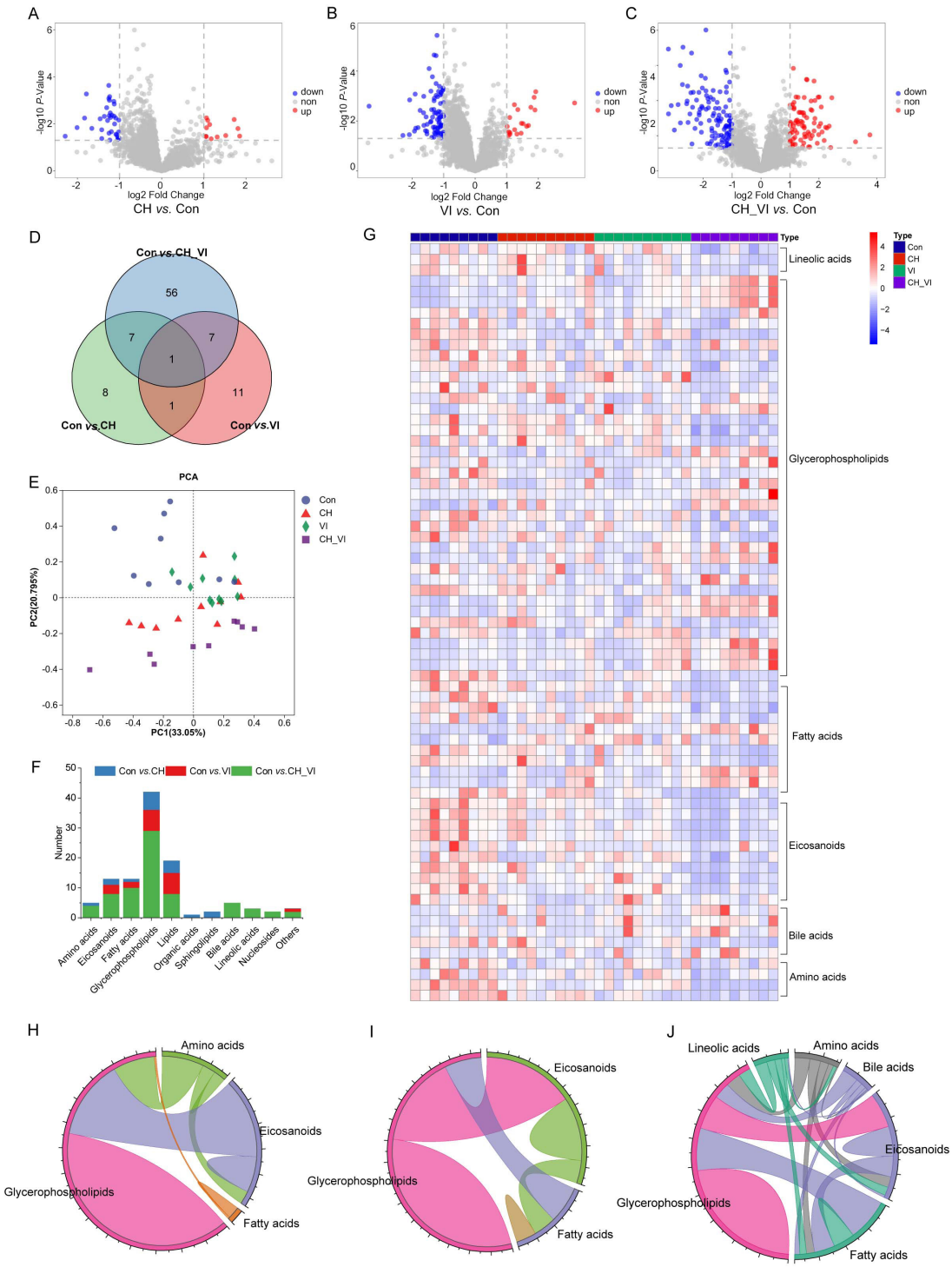

Fig. 6 Metabolome analysis of serum samples. Con, control group; CH, cold humid exposure group; VI, virus infection group; CH_VI, cold humid environment combined with virus infection group. (A-C) Volcano plot showing changes in differential ions between CH, VI, CH_VI and Con group; (D) Venn diagram of DMs in the Con, CH, VI and CH_VI groups; (E) The PCA plots established based on DMs in the Con, CH, VI and CH_VI groups; (F) The categories and number of DMs obtained from the Con, CH, VI and CH_VI groups; (G) Heatmap diagram of DMs in the Con, CH, VI and CH_VI groups; (H) The DMs correlation between major DMs classes in the CH group; (I) The DMs correlation between major DMs classes in the VI group; (J) The DMs correlation between major DMs classes in the CH_VI group.

groups (Fig. 6A–C). Progenesis QI identified a total of 91 DMs based on HMDB, KEGG, LIPIDMAPS, and METLIN databases (Supplementary Table S2) showcasing common and independent DMs among the four groups in Fig. 6D. The PCA model based on these 91 DMs effectively differentiates the four groups (Fig. 6E). While cold exposure and viral infection individually exert limited effects on the serum metabolome, heir simultaneous presence significantly induces blood metabolic disorders in mice, particularly affecting glycerophospholipids, fatty acids, and eicosanoids (Fig. 6F). This outcome is further confirmed by the heatmap based on the obtained DMs (Fig. 6G). Additionally, correlation chord diagrams highlight that cold exposure and viral infection leads to more severe serum metabolome disorders in mice compared to exposure to cold or viral infection alone (Fig. 6H–J).

3.6 Metabolic pathway analysis

To delve into the metabolic pathways affected by cold exposure and viral infection, we performed metabolic pathway enrichment analysis using the KEGG database based on DMs obtained in lung tissue and serum. Pathway enrichment analysis revealed significant enrichment of lipid metabolism and nucleotide metabolism in serum, with 8 lipid metabolic pathways and 2 nucleotide metabolic pathways, respectively (Fig. 7A). Among the lipid metabolic pathways, 3 were related to fatty acid (alpha-linolenic acid metabolism, arachidonic acid metabolism,

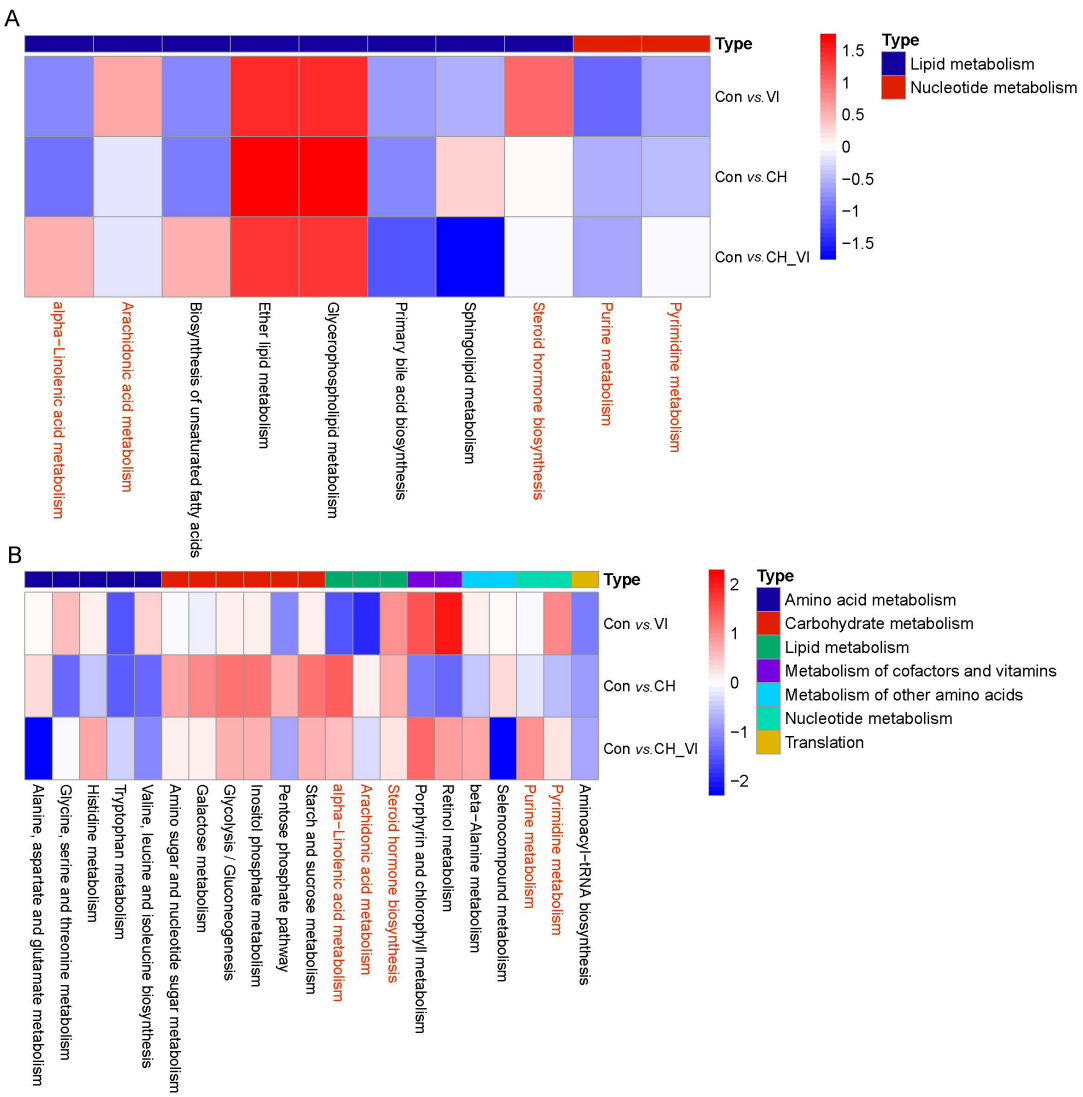

Fig. 7 Pathway enrichment analysis of differential metabolites (DMs) in lung tissue specimens and serum samples. Con, control group; CH, cold humid exposure group; VI, virus infection group; CH_VI, cold humid environment combined with virus infection group. (A) serum; (B) Lung tissue.

biosynthesis of unsaturated fatty acids).

The types of metabolic pathways enriched in lung tissue were more diverse than those in serum, encompassing carbohydrate metabolism (6), amino acid metabolism (5), lipid metabolism (3), metabolism of other amino acids (2), metabolism of cofactors and vitamins (2), and nucleotide metabolism (1) (Fig. 7B). Commonly enriched metabolic pathways in both lung tissue and serum included purine metabolism, pyrimidine metabolism, steroid hormone biosynthesis, arachidonic acid metabolism, and alpha-linolenic acid metabolism. In a published lipidomics study of COVID-19 patients, pathway enrichment also indicated arachidonic acid metabolism, fatty acid biosynthesis, and alpha-linolenic acid metabolism were severely affected biochemical pathway[26]. These results suggest that nucleotide metabolism and lipid metabolism and lipid metabolism, particularly fatty acid metabolism, play pivotal roles in the response to both cold exposure and viral infection.

3.7 Correlation analysis of the gut microbiota-metabolites-inflammatory indicators axis

To identify co-regulated metabolic pathways across tissues, we conducted Spearman correlation analysis and utilized Cytoscape to construct a correlation network based on DMs and immune-inflammation indicators with significant correlations ($P < 0.05$

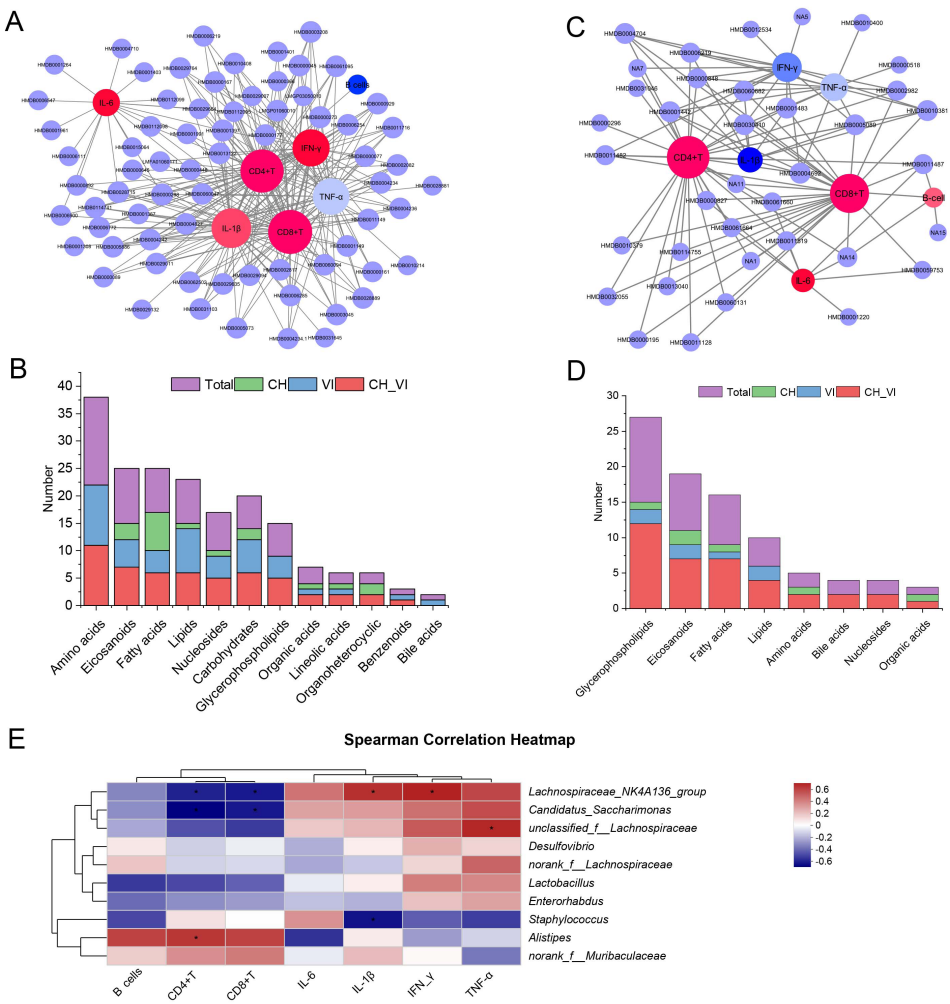

Fig. 8 Correlation analysis. Con, control group; CH, cold humid exposure group; VI, virus infection group; CH_VI, cold humid environment combined with virus infection group. (A) Spearman correlation analysis of differential metabolites (DMs) in lung tissue with immune-inflammatory indicators; (B) The categories and number of significantly ($P < 0.05$ and $|cor| > 0.5$) correlated DMs in lung tissue; (C) Spearman correlation analysis of DMs in serum with immune-inflammatory indicators; (D) The categories and number of significantly ($P < 0.05$ and $|cor| > 0.5$) correlated DMs in serum; (E) Spearman correlation analysis of the gut microbiota with immune-inflammatory indicators. Significance levels are indicated as follows: *, $P < 0.05$.

and |cor| > 0.5). In lung tissue, amino acids, eicosanoids, and fatty acids were predominantly enriched, exhibiting significant correlations with immune-inflammatory indicators, especially $CD4^+$ T cells and $CD8^+$ T cells (Fig. 8A–B). These findings were corroborated in serum, where glycerophospholipids, eicosanoids, and fatty acids were the main enrichment, displaying significantly correlations with immune-inflammatory indicators, especially $CD4^+$ T cells and $CD8^+$ T cells (Fig. 8C–D). The outcomes indicate an indispensable role for lipids in immune system regulation, with cold exposure and viral infection potentially impairing immune function by altering lipid metabolism.

Among the top 10 bacteria, *lachnospiraceae_NK4A136_group*, and unclassified *f_Lachnospiraceae* showed a significant positive correlation ($P < 0.05$) with inflammatory indicators such as IL-1β, IFN-γ, and TNF-α). *Candidatus_Saccharimonas* and *lachnospiraceae_NK4A136_group* displayed a significant negative correlation ($P < 0.05$) with immune cytokines $CD4^+$ T cells and $CD8^+$ T cells. In addition, *Staphylococcus* also showed a significant negative correlation ($P < 0.05$) with IL-1β, while *Alistipes* exhibited a significant positive correlation ($P < 0.05$) with $CD4^+$ T cells (Fig. 8E). Thus, gut microbiota emerges as a pivotal regulator of immune function.

4 Discussion

In our study, we observed typical pulmonary lesions induced by both cold exposure and virus infection, accompanied by an increase in proinflammatory cytokines in the lungs and a decrease in immune cells percentages in peripheral blood. Notably, our results suggested that cold exposure exacerbates the HCoV-229E-induced immune function impairment in mice. This effect is linked to the cold exposure modifying gut microbiota and host lipid metabolism, thereby impairing the immune function of virus-infected mice. Overall, these findings emphasize the unique microbiota-mediated immune responses across the gut-lung axis and various organ sites in mice exposed to the combination of cold and virus infection.

A wealth of evidence points to temperature and humidity as independent or joint factors influencing the risk of respiratory viral infections due to alterations in host susceptibility[27-28]. Recent studies have highlighted that cold temperatures may compromise the host's innate immune response to viral infections[29-30] and impede extracellular vesicle swarm-mediated nasal antiviral immunity[16]. Cold exposure is known to suppress immune responses, leading to decreased lymphocyte proliferation, downregulation of immune cascades, and heightened susceptibility to infections[31]. In our investigation, we observed that cold exposure predominantly impairs the immune system, resulting in a significant decrease in various immune cytokines in $CD4^+$ T cells and $CD8^+$ T cells. Additionally, cold exposure exacerbates immune system damage caused by viral infections.

Accumulating evidence supports the notion that gut microbiota plays a crucial role in regulating both innate and adaptive immune systems[32], closely influencing the severity and prognosis of viral infections[7,10-11]. Previous studies have identified *Firmicutes*, including *Alistipes* and *Staphylococcus*, as pivotal players associated with COVID-19 severity, with *Alistipes* standing out as a top bacterial species negatively correlated with COVID-19 severity[7,33]. *Alistipes*, engaged in tryptophan metabolism for indole derivative production, contributes to maintaining gut immune homeostasis and correlates positively correlated with B cell precursors[34]. Conversely, *Staphylococcus* is frequently linked to adverse patient outcomes[35]. In our study, we found that cold exposure significantly increased the abundance of *Staphylococcus* while decreasing the levels of *Alistipes*, with both bacteria showing significant correlations with immune-inflammatory indicators. Previous research has highlighted the gut microbiota's role in orchestrating energy homeostasis during cold exposure[15,36]. Cold exposure triggers intense physiological reactions, including peripheral vasoconstriction and shivering thermogenesis, aiming to balance heat dissipation and generation[37]. The pro-inflammatory immune response, considered a high-cost, high-benefit trait, becomes vulnerable to environmental changes that can shift cost-benefit balances[38]. To sustain immune system homeostasis during inflammation, a substantial number of immune cells are generated, demanding a significant amount of metabolic resources[5]. In our study, purine metabolism and pyrimidine metabolism are significantly enriched metabolic pathways during cold exposure. These pathways are mediated by key molecules involved in nucleotide synthesis, control intracellular energy homeostasis, and participate in the body's immune-inflammatory response[39-41]. Currently, it is well-established that the gut microbiota regulates purine metabolite levels, thereby influencing its control over the immune system[42-43]. Therefore, we speculate that cold exposure impairs gut microbiota homeostasis in mice, decreasing immunity and exacerbating the deterioration of the immune system due to viral infection.

As crucial as gut microbiota, host metabolites also play an irreplaceable role in virus transmission and infection. In the serum and lung tissue metabolome, cold exposure significantly affected glycerophospholipids, fatty acids, and eicosanoids. The alterations in serum glycerophospholipids, fatty acids, and eicosanoids were more pronounced in virus-infected mice exposed to a cold environment than in mice exposed to cold alone or virus-infected mice alone. Studies indicate that viral infection induces substantial changes in host cells lipids, exploiting key energy pathways and fueling various stages of viral infection[44]. Previous comprehensive untargeted metabolomic

and lipidomic analyses of the host's response to SARS-CoV-2 infection revealed significant disturbances in fatty acid metabolism, glycerophospholipids metabolism, and amino acid metabolism[45-46]. Glycerophospholipids, a key class of signaling molecules, exhibit diverse biological activities, participating in cell growth, apoptosis, plasma membrane formation, and inflammatory responses in cell and tissue metabolism[47-48]. They also engage in metabolic pathways and regulatory mechanisms shared with leukotrienes, thromboxanes, and prostaglandins, constituting a novel class of inflammatory lipids[49]. Fatty acids serve as building blocks for membrane synthesis during viral proliferation and can be converted into lipid mediators, such as eicosanoids, playing pivotal roles in immune and inflammatory processes[26]. Furthermore, our observations revealed a robust correlation between glycerophospholipids, fatty acids, eicosanoids, and immune-inflammatory indicators.

To sum up, cold exposure induces gut microbiota imbalance in mice, characterized by a reduction in the abundance of beneficial bacteria *Alistipes* and an increase in the abundance of pathogenic bacteria *Staphylococcus*. The disruption in gut microbiota cascades into metabolic disorders in both serum and lung tissue through the "gut-lung" axis, ultimately resulting in compromised immune function in mice. Consequently, this exacerbates the impact of viral infection on the immune system of mice, as illustrated in Fig. 9. While our study establishes an association between gut microbiota and metabolic disorders triggered by cold exposure and viral infection, it comes with certain limitations. Firstly, while existing research indicates the significant role of gut microbiota in cold exposure promoting viral infection, a deeper understanding of how specific gut bacteria contribute to the interaction with viral infection on the immune system requires further elucidation. Secondly, confirming the causal link between cold exposure and the gut microbiome interaction necessitates additional research, including experiments such as fecal microbiota transplantation and specific bacterial treatment. Nevertheless, our findings establish a direct link between cold expose-induced gut microbiota dysregulation and viral infection.

5 Conclusion

In conclusion, our study reveals that the gut microbiota imbalance induced by cold exposure is intricately linked to the severity of viral infection. Cold exposure not only diminishes

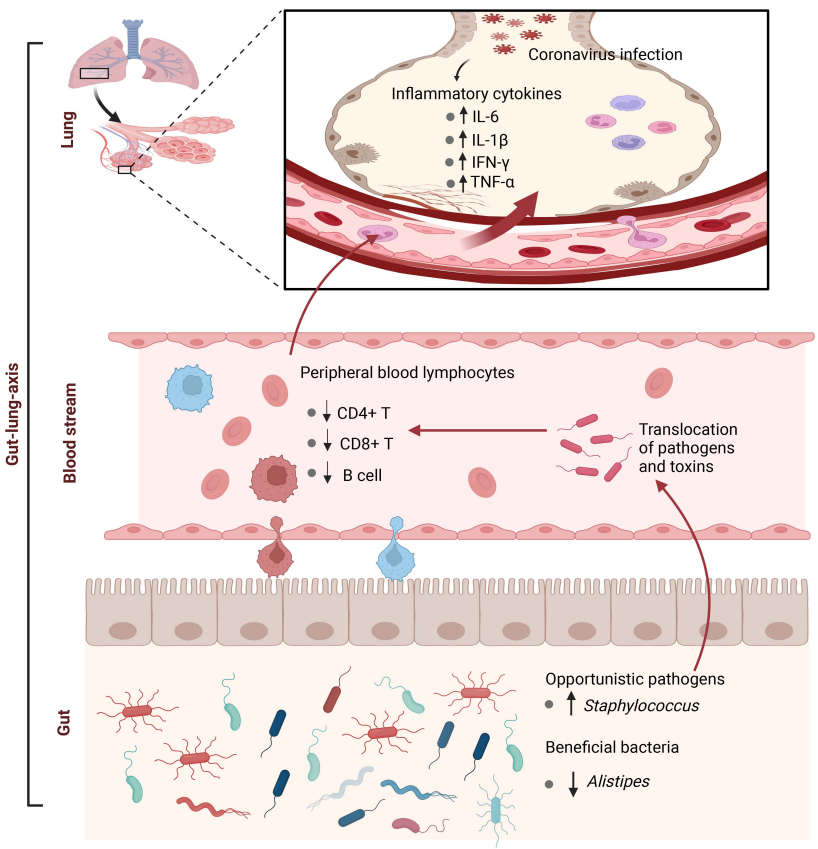

Fig. 9 The possible mechanisms by which cold exposure promotes coronavirus infection.

the abundance and diversity of gut microbiota but also alters its structure, exemplified by a significant increase in potential pathogenic bacteria such as *staphylococcus* and a notable decrease in beneficial bacteria like *Alistipes*. The resultant disturbance in gut microbiota triggers metabolic disorders associated with immune function, thereby intensifying the detrimental impact of viral infection on the immune system. This newfound understanding of the interplay between gut microbiota, cold exposure, and coronavirus infection contributes valuable insights for the prevention and treatment of diseases stemming from coronavirus infections, particularly for individuals working outdoors in cold environments.

Acknowledgments

The work was supported by the National Key Research and Development Program of China (2020YFC0845400). National Natural Science Foundation of China (82141203, 82304753), Innovation Team and Talents Cultivation Program of National Administration of Traditional Chinese Medicine (ZYYCXTD-D-202004), and Shanghai Frontiers Science Center of TCM Chemical Biology. We are very grateful to Professor Xiaolan Cui and her team from the China Academy of Chinese Medical Sciences for their support in animal models.

Ethics approval and consent to participate

The study was approved and monitored by the Animal Care and Use Committee of the Institute of Chinese Materia Medica, China Academy of Chinese Medical Sciences (2020D028).

Data availability statement

Data will be made available from the corresponding author Zhang W D, upon reasonable request.

Conflict of interest

Zhang W D is an Editorial Board Member of Frigid Zone Medicine. The article was subject to the journal's standard procedures, with peer review handled independently of this Member and his research groups. The authors declare that the research was conducted in the absence of any commercial or financial relationships that could be construed as a potential conflict of interest.

Authorship contribution

Zhang W D and Li H K co-supervised this research project. Wu G S and Zhang Y H analyzed the data and drafted this manuscript. Zheng N N, Tian S S, Liao J Y and Le W Q helped analyze the data. All authors contributed to the article and approved its submission at the present form.

Supplementary Material

The Supplementary Material for this article can be found online.

References

[1] Abdelrahman Z, Li M, Wang X. Comparative review of sars-cov-2, sars-cov, mers-cov, and influenza a respiratory viruses. Front Immunol, 2020; 11: 552909.
[2] Karki R, Lee S, Mall R, *et al.* Zbp1-dependent inflammatory cell death, panoptosis, and cytokine storm disrupt ifn therapeutic efficacy during coronavirus infection. Sci Immunol, 2022; 7(74): eabo6294.
[3] Abid M B, Mughal M, Abid M A. Coronavirus disease 2019 (covid-19) and immune-engaging cancer treatment. JAMA Oncol, 2020; 6(10): 1529-1530.
[4] Ye L, Jiang Y, Zhang M. Crosstalk between glucose metabolism, lactate production and immune response modulation. Cytokine Growth Factor Rev, 2022; 68: 81-92.
[5] Spiljar M, Steinbach K, Rigo D, *et al.* Cold exposure protects from neuroinflammation through immunologic reprogramming. Cell Metab, 2021; 33 (11): 2231-2246.e8.
[6] Dai H, Tang H, Sun W, *et al.* It is time to acknowledge coronavirus transmission *via* frozen and chilled foods: Undeniable evidence from china and lessons for the world. Sci Total Environ, 2023; 868: 161388.
[7] Zuo T, Zhang F, Lui G C Y, *et al.* Alterations in gut microbiota of patients with covid-19 during time of hospitalization. Gastroenterology, 2020; 159(3): 944-955.e8.
[8] Liu Q, Mak J W Y, *et al.* Gut microbiota dynamics in a prospective cohort of patients with post-acute covid-19 syndrome. Gut, 2022; 71(3): 544-552.
[9] Ren Z, Wang H, Cui G, *et al.* Alterations in the human oral and gut microbiomes and lipidomics in covid-19. Gut, 2021; 70(7): 1253-1265.
[10] Yeoh Y K, Zuo T, Lui G C, *et al.* Gut microbiota composition reflects disease severity and dysfunctional immune responses in patients with covid-19. Gut, 2021; 70(4): 698-706.
[11] Nagata N, Takeuchi T, Masuoka H, *et al.* Human gut microbiota and its metabolites impact immune responses in covid-19 and its complications. Gastroenterology, 2023; 164(2): 272-288.
[12] Katz-Agranov N, Zandman-Goddard G. Autoimmunity and covid-19 - the microbiotal connection. Autoimmun Rev, 2021; 20(8): 102865.
[13] Sun Z, Song Z G, Liu C, *et al.* Gut microbiome alterations and gut barrier dysfunction are associated with host immune homeostasis in

covid-19 patients. BMC Med, 2022; 20(1): 24.
[14] Vatanen T, Kostic A D, d'Hennezel E, *et al.* Variation in microbiome lps immunogenicity contributes to autoimmunity in humans. Cell, 2016; 165(4): 842-853.
[15] Chevalier C, Stojanovic O, Colin D J, *et al*. Gut microbiota orchestrates energy homeostasis during cold. Cell, 2015; 163(6): 1360-1374.
[16] Huang D, Taha M S, Nocera A L, *et al.* Cold exposure impairs extracellular vesicle swarm-mediated nasal antiviral immunity. J Allergy Clin Immunol, 2023; 151(2): 509-525.e8.
[17] Tian S, Zheng N, Zu X, *et al.* Integrated hepatic single-cell rna sequencing and untargeted metabolomics reveals the immune and metabolic modulation of qing-fei-pai-du decoction in mice with coronavirus-induced pneumonia. Phytomedicine, 2022; 97: 153922.
[18] Wu G, Zhang W, Zheng N, *et al.* Integrated microbiome and metabolome analysis reveals the potential therapeutic mechanism of qing-fei-pai-du decoction in mice with coronavirus-induced pneumonia. Front Cell Infect Microbiol, 2022; 12: 950983.
[19] Gilbert J A, Blaser M J, Caporaso J G, *et al.* Current understanding of the human microbiome. Nat Med, 2018; 24(4): 392-400.
[20] Parker B J, Wearsch P A, Veloo A C M, *et al.* The genus *Alistipes*: Gut bacteria with emerging implications to inflammation, cancer, and mental health. Front Immunol, 2020; 11: 906.
[21] Broker B M, Holtfreter S, Bekeredjian-Ding I. Immune control of *Staphylococcus* aureus - regulation and counter-regulation of the adaptive immune response. Int J Med Microbiol, 2014; 304(2): 204-214.
[22] Tsai C M, Caldera J R, Hajam I A, *et al.* Non-protective immune imprint underlies failure of *Staphylococcus* aureus isdb vaccine. Cell Host Microbe, 2022; 30(8): 1163-1172.e6.
[23] Zheng L, Kelly C J, Battista K D, *et al.* Microbial-derived butyrate promotes epithelial barrier function through il-10 receptor-dependent repression of claudin-2. J Immunol, 2017; 199(8): 2976-2984.
[24] Klaring K, Just S, Lagkouvardos I, *et al*. Murimonas intestini gen. Nov., sp. Nov., an acetate-producing bacterium of the family lachnospiraceae isolated from the mouse gut. Int J Syst Evol Microbiol, 2015; 65(Pt 3): 870-878.
[25] Yusufu I, Ding K, Smith K, *et al.* A tryptophan-deficient diet induces gut microbiota dysbiosis and increases systemic inflammation in aged mice. Int J Mol Sci, 2021; 22(9): 5005.
[26] Castane H, Iftimie S, Baiges-Gaya G, *et al.* Machine learning and semi-targeted lipidomics identify distinct serum lipid signatures in hospitalized covid-19-positive and covid-19-negative patients. Metabolism, 2022; 131: 155197.
[27] Ikaheimo T M, Jaakkola K, Jokelainen J, *et al*. A decrease in temperature and humidity precedes human rhinovirus infections in a cold climate. Viruses, 2016; 8(9): 244.
[28] Jaakkola K, Saukkoriipi A, Jokelainen J, *et al.* Decline in temperature and humidity increases the occurrence of influenza in cold climate. Environ Health, 2014; 13(1): 22.
[29] Foxman E F, Storer J A, Fitzgerald M E, *et al*. Temperature-dependent innate defense against the common cold virus limits viral replication at warm temperature in mouse airway cells. Proc Natl Acad Sci U S A, 2015; 112(3): 827-832.
[30] Foxman E F, Storer J A, *et al.* Two interferon-independent double-stranded rna-induced host defense strategies suppress the common cold virus at warm temperature. Proc Natl Acad Sci U S A, 2016; 113(30): 8496-8501.
[31] Shephard R J, Shek P N. Cold exposure and immune function. Can J Physiol Pharmacol, 1998; 76(9): 828-836.
[32] Zheng D, Liwinski T, Elinav E. Interaction between microbiota and immunity in health and disease. Cell Res, 2020; 30(6): 492-506.
[33] Garcia-Vidal C, Sanjuan G, Moreno-Garcia E, *et al.* Incidence of co-infections and superinfections in hospitalized patients with covid-19: A retrospective cohort study. Clin Microbiol Infect, 2021; 27(1): 83-88.
[34] Gao J, Xu K, Liu H, *et al.* Impact of the gut microbiota on intestinal immunity mediated by tryptophan metabolism. Front Cell Infect Microbiol, 2018; 8: 13.
[35] Mulcahy M E, McLoughlin R M. *Staphylococcus* aureus and influenza a virus: Partners in coinfection. mBio, 2016; 7(6): e02068-16.
[36] Zhang X Y, Sukhchuluun G, Bo T B, *et al.* Huddling remodels gut microbiota to reduce energy requirements in a small mammal species during cold exposure. Microbiome, 2018; 6(1): 103.
[37] Walsh N P, Whitham M. Exercising in environmental extremes : A greater threat to immune function? Sports Med, 2006; 36(11): 941-976.
[38] Okin D, Medzhitov R. Evolution of inflammatory diseases. Curr Biol, 2012; 22(17): R733-40.
[39] Huang Z, Xie N, Illes P, *et al.* From purines to purinergic signalling: Molecular functions and human diseases. Signal Transduct Target Ther, 2021; 6(1): 162.
[40] Longhi M S, Moss A, Jiang Z G, *et al.* Purinergic signaling during intestinal inflammation. J Mol Med (Berl), 2017; 95(9): 915-925.
[41] Yang R, Yang C, Ma L, *et al.* Identification of purine biosynthesis as an nadh-sensing pathway to mediate energy stress. Nat Commun, 2022; 13(1): 7031.
[42] Wu J, Wei Z, Cheng P, *et al*. Rhein modulates host purine metabolism in intestine through gut microbiota and ameliorates experimental colitis. Theranostics, 2020; 10(23): 10665-10679.
[43] Mager L F, Burkhard R, Pett N, *et al.* Microbiome-derived inosine modulates response to checkpoint inhibitor immunotherapy. Science, 2020; 369(6510): 1481-1489.
[44] Bley H, Schobel A, Herker E. Whole lotta lipids-from hcv rna replication to the mature viral particle. Int J Mol Sci, 2020; 21(8): 2888.
[45] Song J W, Lam S M, Fan X, *et al*. Omics-driven systems interrogation of metabolic dysregulation in covid-19 pathogenesis. Cell Metab, 2020; 32(2): 188-202 e5.
[46] Barberis E, Timo S, Amede E, *et al.* Large-scale plasma analysis revealed new mechanisms and molecules associated with the host response to sars-cov-2. Int J Mol Sci, 2020; 21(22): 8623.
[47] Makide K, Kitamura H, Sato Y, *et al*. Emerging lysophospholipid mediators, lysophosphatidylserine, lysophosphatidylthreonine, lysophosphatidylethanolamine and lysophosphatidylglycerol. Prostaglandins Other Lipid Mediat, 2009; 89(3-4): 135-139.
[48] Shindou H, Hishikawa D, Harayama T, *et al*. Generation of membrane diversity by lysophospholipid acyltransferases. J Biochem, 2013; 154(1): 21-28.
[49] Sevastou I, Kaffe E, Mouratis M A, *et al.* Lysoglycerophospholipids in chronic inflammatory disorders: The pla(2)/lpc and atx/lpa axes. Biochim Biophys Acta, 2013; 1831(1): 42-60.